Research Square

Preprints are preliminary reports that have not undergone peer review.
They should not be considered conclusive, used to inform clinical practice,
or referenced by the media as validated information.

Time-specific associations of TP53 mutation and CDKN2A deletion with treatment failure in diffuse large B-cell lymphoma

jinliang zhang

13148049308@163.com

National Cancer Center/National Clinical Research Center for Cancer/Cancer Hospital, Chinese Academy of Medical Sciences and Peking Union Medical College https://orcid.org/0009-0005-7984-2247

fanshuang zhang

National Cancer Center/National Clinical Research Center for Cancer/Cancer Hospital, Chinese Academy of Medical Sciences and Peking Union Medical College

yiluo liu

National Cancer Center/National Clinical Research Center for Cancer/Cancer Hospital, Chinese Academy of Medical Sciences and Peking Union Medical College

xuejian cui

National Cancer Center/National Clinical Research Center for Cancer/Cancer Hospital, Chinese Academy of Medical Sciences and Peking Union Medical College

zitong feng

National Cancer Center/National Clinical Research Center for Cancer/Cancer Hospital, Chinese Academy of Medical Sciences and Peking Union Medical College

Xuemin Xue

National Cancer Center/National Clinical Research Center for Cancer/Cancer Hospital, Chinese Academy of Medical Sciences and Peking Union Medical College https://orcid.org/0000-0002-7842-6883

Xiaoli Feng

National Cancer Center/National Clinical Research Center for Cancer/Cancer Hospital

jianming ying

National Cancer Center/National Clinical Research Center for Cancer/Cancer Hospital, Chinese Academy of Medical Sciences and Peking Union Medical College

tian qiu

National Cancer Center/National Clinical Research Center for Cancer/Cancer Hospital, Chinese Academy of Medical Sciences and Peking Union Medical College

Article

Keywords: diffuse large B-cell lymphoma, TP53, CDKN2A, treatment failure, prognostic biomarkers

Posted Date: November 23rd, 2026

DOI: https://doi.org/10.21203/rs.3.rs-11692013/v1

License: This work is licensed under a Creative Commons Attribution 4.0 International License.
Read Full License

Additional Declarations: There is **NO** conflict of interest to disclose.

Abstract

Roughly one third of patients with diffuse large B-cell lymphoma (DLBCL) are not cured by first-line immunochemotherapy, but the genetic determinants of when treatment fails remain unresolved. We analysed 822 patients with DLBCL, of whom 484 responded to first-line therapy, and modelled failure in defined windows, each on its own risk set. *TP53* mutation (99 patients, 20.5%) was associated with failure in the first 12 months (hazard ratio [HR] 2.27, 95% CI 1.28–4.02, $P = 0.005$) and not thereafter (12–24 months: HR 0.93). *CDKN2A* loss (72 patients, 14.9%) showed the reverse profile: no association in the first year (HR 1.38) and a strong association between 12 and 24 months (HR 4.58, 95% CI 1.96–10.73, $P < 0.001$). The two lesions were mutually exclusive (3 co-occurrences vs 14.7 expected; odds ratio 0.14, 95% CI 0.04–0.46), and this was reproduced in four external datasets. Disruption of the axis by either lesion predicted failure in both windows (HR 2.02 and 3.08), and the identity of the lesion determined the timing. These findings define two failure clocks within one pathway and a time-specific framework for interpreting *TP53* and *CDKN2A* status in DLBCL.

Introduction

First-line immunochemotherapy cures most patients with diffuse large B-cell lymphoma (DLBCL), but 30–40% do not respond or relapse, and failure within the first year accounts for most disease-related mortality [1, 2]. Failure timing is already embedded in clinical practice: event-free survival at 24 months is a robust surrogate [3], early relapse is a trial eligibility or stratification criterion [4], and late relapse frequently arises from a genetically distinct clone, with primary refractoriness arising from the diagnostic clone [5].

The molecular determinants of when failure occurs remain unclear because the lesions that predict adverse outcome are studied as a set. Three lesions dominate the axis: *TP53* mutation, *CDKN2A* copy-number loss and *MYC* rearrangement. Each is individually adverse [6–9]; the A53 cluster of the LymphGen classification, which assigns many cases to genetically defined subtypes, is defined by *TP53* inactivation [10, 11], and a pooled analysis found *TP53* and *CDKN2A* lesions enriched in patients who failed within two years [12]. They are therefore usually reported as one aggregate high-risk signal, without regard to when the risk falls.

Two observations suggest that this aggregation discards information. The lesions are not distributed independently: *CDKN2A* deletion and *TP53* mutation are mutually exclusive in MCD DLBCL [13], whereas an earlier, smaller study reported them as independent [14]. In Barrett's oesophagus, *CDKN2A* loss counter-selects subsequent *TP53* loss during clonal evolution [15], which places the two events on distinct routes. Distinct routes need not fail at the same time.

We therefore asked whether lesion type determines the timing of failure in patients who respond to first-line immunochemotherapy, using window-specific models in which each window is analysed on its own risk set.

Methods

Patients and cohort construction

The study cohort comprised 1,082 samples from 1,059 unique patients with molecular data; of 828 patients with a diagnosis of DLBCL, 822 had an available first-line treatment record with molecular data. All patients received first-line immunochemotherapy; R-CHOP or R-CHOP-like regimens predominated. Response was recorded based on the treating physician's assessment. Patients with complete response (CR), partial response (PR), stable disease (SD), or progressive disease (PD) were considered evaluable for response (n = 536). The primary analysis set comprised the 484 responders (CR/PR), because the question concerned failure after an initial response; the 52 patients with primary treatment refractoriness (PD/SD) were not included in the window analyses.

Molecular assessment

TP53 mutation was determined by targeted next-generation sequencing of lymphoma tissue and was analysed as a binary variable (any non-synonymous variant at variant allele frequency ≥ 0.10). *CDKN2A* copy number was derived from a sample-level copy-number matrix and analysed as a binary variable (loss versus no loss). The copy-number call carries a confidence annotation that distinguishes homozygous deletion (cnv_confidence_level − 2) from heterozygous deletion (− 1); amplification and no-alteration calls were both coded as no loss. The composition of the loss group and window-specific sensitivity analyses restricted to homozygous or to heterozygous deletion are given in Table S1. *MYC* rearrangement, *BCL2* rearrangement and *BCL6* rearrangement were determined by fluorescence in situ hybridisation. "Single-hit *MYC*" denotes *MYC* rearrangement without a concurrent *BCL2* or *BCL6* rearrangement; "double-hit lymphoma" (DHL) denotes concurrent *MYC* and *BCL2* and/or *BCL6* rearrangement. Cell of origin was assigned by the Hans algorithm using CD10, MUM1 and *BCL6* immunohistochemistry. *MYD88*, *CD79B* and other gene mutations were called at variant allele frequency ≥ 0.10; "MCD-like" denotes the presence of any *MYD88* or *CD79B* mutation. p53 immunohistochemistry was scored as the fraction of tumour cells with strong nuclear positivity. LymphGen subtypes were approximated with a rule-based classifier using mutation and copy-number features and used only for stratification. Double-expressor lymphoma (DEL) was defined as concurrent expression of the *MYC* and *BCL2* proteins by immunohistochemistry (≥ 40% and ≥ 50% of tumour cells, respectively). Ki-67 was recorded as the percentage of tumour cells with nuclear positivity.

Statistical analysis

The central methodological choice was to analyse failure in clinically defined windows, with each window modelled on its own risk set. For a window from l to h months, a patient contributed follow-up only if they remained at risk at l (that is, follow-up exceeded l), time was rescaled as $\min(t, h) - l$, and an event was counted only if it occurred at or before h. This segmented (piecewise) construction prevents an event occurring after the window from being attributed to it, and prevents patients who have already

left the risk set from contributing to a later window. We analysed the windows 0–6, 6–12, 12–18, 18–24, 0–12, 12–24, 0–18 and 18–36 months. The primary contrasts were *TP53* mutation in 0–12 months and *CDKN2A* loss in 12–24 months.

Effects are expressed as hazard ratios (HR) with 95% confidence intervals from Cox proportional-hazards models [16] without penalisation; a ridge penalizer of 0.05 was applied only where the likelihood was separated (single-hit *MYC* in the 18–24-month window, flagged in the source data). Cumulative incidence was estimated by the Kaplan–Meier method [17]. Multivariable models included age ≥ 60 years, male sex, non-GCB cell of origin, and — in a separate complete-case analysis — International Prognostic Index (IPI) ≥ 3 and Ann Arbor stage III–IV. Subtype-adjusted models used Cox models stratified by approximated LymphGen subtype.

Tests of time-specificity

We tested whether the effect differed between windows using a counting-process (person-period) Cox model fitted to the interval 0–24 months, in which each patient's follow-up is split at 12 months and a lesion-by-window product term gives the ratio of the late-window to the early-window hazard ratio. A window indicator is a deterministic function of the time scale and is therefore absorbed by the non-parametric baseline hazard; it was not entered as a separate term, and no penalisation was applied. The same quantity was also formed as the ratio of the late-window to the early-window HR from the two separately estimated window models and tested with the standard error of the difference of the two log-HRs; it returned an identical estimate. To test whether the two lesions differ in when they act, both lesions and both lesion-by-window product terms were entered into a single model and the two product terms compared directly.

Multiplicity

The four lesion-by-primary-window combinations were treated as the primary family and controlled by the Benjamini–Hochberg procedure and by Bonferroni correction. All 24 lesion-by-window combinations were also examined with Benjamini–Hochberg control to place the primary results in context.

Specificity and robustness

Specificity was assessed by screening every available marker (15 immunohistochemical and copy-number variables) and every mutated gene with sufficient frequency (38 genes) against both primary windows, with Benjamini–Hochberg control of the false discovery rate. Robustness was assessed by bootstrap resampling (500 replicates), permutation of lesion labels (1 000 permutations), and leave-one-out analysis.

Odds ratios for co-occurrence of *TP53* mutation and *CDKN2A* loss were computed by Fisher's exact test, always within the same set of patients in whom both variables were measured. Co-occurrence was

estimated separately in each cohort, and heterogeneity was assessed by Cochran's Q.

Survival endpoint

Progression-free survival in this registry is recorded as time to progression or relapse; deaths were not captured as events. The endpoint analysed here is therefore strictly time to progression or relapse, and is referred to as "failure" throughout.

Analyses used Python 3 with pandas, NumPy, SciPy and lifelines. Two-sided *P* values < 0.05 were considered significant.

External datasets

Four public datasets were analysed from cBioPortal [18] using a uniform definition of *CDKN2A* copy-number loss (any loss) and *TP53* mutation: dlbcl_duke_2017 (Reddy et al., n = 1 001) [19], mbn_msk_2024 (Zhu et al., n = 396) [20], dlbc_tcga_pan_can_atlas_2018 (TCGA PanCancer Atlas, n = 48) [10, 21] and pcnsl_msk_2024 (Grommes et al., n = 86) [22]. These datasets were used only to test the co-occurrence relationship; no survival analysis was performed on them. Datasets differ in assay (whole-exome sequencing with log2 copy-number ratios for Duke/Reddy; targeted panels with discrete GISTIC calls for the remainder), which is the principal source of between-cohort heterogeneity.

Results

Cohort

Of 1 082 samples from 1 059 patients with molecular data, 822 patients had DLBCL and a first-line treatment record (Fig. 1A). Median follow-up in the 484 responders was 14.0 months, with 52.7% followed beyond 12 months and 141 patients beyond 24 months (Fig. 1C). Fifty-two patients (10.7%) failed within 12 months and a further 22 failed between 12 and 24 months among 255 patients still at risk (8.6%; Supplementary Table S2).

TP53 mutation was present in 99 of 484 responders (20.5%) and single-hit *MYC* in 17 (3.5%); DHL was present in 15 (3.1%). *CDKN2A* copy number was available for all 484 responders, of whom 72 (14.9%) had loss. *CDKN2A* status could be analysed in every responder because the copy-number matrix reports only altered samples (Methods). Baseline characteristics are shown in Table S3. Ki-67 was higher in *CDKN2A*-deleted patients (median 85% vs 80%, *P* = 0.025), and DEL was more frequent (29.2% vs 14.6%, *P* = 0.011); adjustment for DEL left both lesion effects essentially unchanged (hazard ratios 3.21 and 4.45). IPI was available in 361 of 484 patients (74.6%) and Ann Arbor stage in 400 (82.6%).

Lesion type and the failure window

Segmented Cox analysis of the three principal lesions produced three different temporal profiles (Fig. 2A). *TP53* mutation was associated with failure in the first year (0–12 months: HR 2.27, 95% CI 1.28–4.02, $P = 0.005$) with no association thereafter (12–24 months: HR 0.93, 95% CI 0.32–2.75, $P = 0.90$). *CDKN2A* loss showed the reverse profile: no association with failure in the first year (0–12 months: HR 1.38, 95% CI 0.69–2.75, $P = 0.36$) and a strong association with failure between 12 and 24 months (HR 4.58, 95% CI 1.96–10.73, $P < 0.001$). Single-hit *MYC* was intermediate in both timing and strength, reaching significance in the pooled 0–18-month window (HR 3.46, 95% CI 1.58–7.58, $P = 0.002$).

The corresponding cumulative incidence curves cross (Fig. 2B): by 12 months 22.7% of *TP53*-mutated patients had failed, compared with 14.0% of patients whose dominant lesion was *CDKN2A* deletion; by 24 months the positions had reversed (29.9% vs 37.9%). In patients in whom no lesion was detected, cumulative failure was 10.3% at 12 months and 15.8% at 24 months.

Restricting the analysis to the narrower windows that make up the primary ones localised the effects further (Fig. 2A; the complete 3 × 8 grid is given in Table S4). For *TP53*, the association was already present at 0–6 months and persisted (0–6 months: HR 2.33, 95% CI 1.03–5.27, $P = 0.043$; 6–12 months: HR 2.21, $P = 0.051$), with no signal in 12–18 (HR 0.77, $P = 0.73$) or 18–24 months (HR 1.19, $P = 0.83$). For *CDKN2A*, no window beginning before 12 months was significant (0–6 months: HR 1.76, $P = 0.23$; 6–12 months: HR 1.04, $P = 0.94$; 0–12 months: HR 1.38, $P = 0.36$), and both windows beginning at 12 months were significant (12–18 months: HR 9.89, 95% CI 3.23–30.25, $P < 0.001$; 12–24 months: HR 4.58, 95% CI 1.96–10.73, $P < 0.001$); the 18–24-month band was null (HR 0.92, $P = 0.93$). The 12–18-month band carries the larger point estimate and differs from the 18–24-month band (HR ratio 10.8, 95% CI 1.02–114.4, $P = 0.048$). It rests on 8 events among 38 *CDKN2A*-deleted patients (21.1%) against 5 among 217 *CDKN2A*-retained patients (2.3%; risk difference 18.7%, 95% CI 5.6–31.9) in the same band, and on 1 among 23 in the following six months. The *CDKN2A* effect is concentrated in the second year, with its largest component in the 12–18-month band.

Time-specificity of the two associations

We tested the lesion-by-window interaction directly. In a counting-process Cox model over 0–24 months with a lesion-by-window product term, the interaction HR was 0.41 (95% CI 0.12–1.40, $P = 0.16$) for *TP53* and 3.32 (95% CI 1.11–9.94, $P = 0.032$) for *CDKN2A*. The ratio of late-window to early-window HRs from the two separately fitted window models gave 0.41 (95% CI 0.12–1.38, $P = 0.15$) for *TP53* and 3.32 (95% CI 1.11–9.92, $P = 0.032$) for *CDKN2A*, in close agreement. The *CDKN2A* contrast reaches the conventional threshold; the *TP53* contrast does not. The *TP53* estimate rests on 52 early and 22 late events, four of the latter in *TP53*-mutated patients, giving a resolution of about 5.7-fold for *TP53* and 4.8-fold for *CDKN2A* at 80% power (Figure S1C); the observed ratios were 0.41 (a 2.4-fold difference between the windows) and 3.32.

We next asked whether the two lesions differ in when they act. Entering both lesions and both lesion-by-window product terms into a single model, the ratio of the *TP53* interaction HR to the *CDKN2A* interaction

HR was 0.19 (95% CI 0.04–0.83, *P* = 0.027); the same contrast formed from the separately fitted window models was 0.12 (95% CI 0.02–0.64, *P* = 0.012). The two timing effects therefore differed significantly.

Multiplicity

The primary hypotheses met the criteria: Benjamini–Hochberg false discovery rates of 0.0018 (*CDKN2A* 12–24 months) and 0.0099 (*TP53* 0–12 months) across the four-test primary family (Table S5), and both passed Bonferroni correction (0.0018 and 0.0199). Across the 24 lesion-by-window combinations, five tests survived 5% false-discovery-rate control (Table S4).

The entry route sets the late timing

Axis disruption — the presence of either lesion — was present in 168 of 484 responders (34.7%) and predicted failure in both windows (0–12 months: HR 2.02, 95% CI 1.17–3.47, *P* = 0.011; 12–24 months: HR 3.08, 95% CI 1.32–7.21, *P* = 0.009). The route of disruption determined when that risk fell. Within the 168 patients, the *TP53* route carried the early risk (0–12 months: HR 1.70, 95% CI 0.74–3.92, *P* = 0.21) and the *CDKN2A*-only route carried the late risk (12–24 months: HR 0.30 for the *TP53* route, 95% CI 0.09–0.98, *P* = 0.045; 4 late failures among the 99 *TP53*-route patients versus 9 among the 69 *CDKN2A*-only patients (51 and 37 patients were at risk beyond 12 months)). A single binary axis term therefore captures that failure will occur; the route captures when (Fig. 3B). This is the formal counterpart of the timing difference between the two lesions (*P* = 0.027 in the joint model).

The pattern holds across genetic subtype and cell of origin

CDKN2A loss is closely associated with the MCD genotype [13], so the late window could simply mark MCD biology. Approximated LymphGen subtype did not predict failure timing: failure rates across subtypes were similar in all six windows examined (Fig. 4A; χ^2 *P* = 0.24 to 0.64). Stratifying the Cox models by subtype left the lesion effects essentially unchanged: *TP53* 0–12 months HR 2.27 to 2.31 (95% CI 1.30–4.09, *P* = 0.004); *CDKN2A* 12–24 months HR 4.58 to 5.08 (95% CI 2.08–12.43, *P* < 0.001) (Fig. 4B). The pattern also replicated within cell-of-origin strata: among non-GCB patients, *TP53* mutation predicted early failure (0–12 months: HR 2.42, 95% CI 1.13–5.17, *P* = 0.022) and *CDKN2A* loss predicted late failure (12–24 months: HR 3.48, 95% CI 1.24–9.78, *P* = 0.018); in GCB patients the *CDKN2A* late-window effect was also present (HR 7.80, 95% CI 1.29–46.98, *P* = 0.025) and the *TP53* early-window effect was borderline (HR 3.05, 95% CI 1.00–9.32, *P* = 0.051) (Fig. 4C).

Exclusivity reproduces across independent cohorts and outside MCD

Among the 484 responders, *TP53* mutation and *CDKN2A* loss co-occurred in 3 patients, against 14.7 expected under independence (OR 0.14, 95% CI 0.04–0.46, *P* < 0.001). Because the original description of this exclusivity was restricted to the MCD subtype [13], we tested it in four independent public datasets. No cohort showed a positive association (Fig. 5A; Supplementary Table S6): Duke/Reddy 2017

(n = 1 001) OR 0.50 (0.26–0.96); MSK DLBCL 2024 (n = 396) OR 0.29 (0.15–0.56); TCGA DLBCL (n = 48) and MSK PCNSL 2024 (n = 86) contained no co-occurrence at all. The odds ratios were lowest in this cohort and closest to unity in Duke/Reddy 2017.

Within our own cohort the exclusivity was not restricted to MCD. Using all 484 patients, it was present in MCD-like patients (any *MYD88* or *CD79B* mutation; n = 155; OR 0.28, *P* = 0.051) and no co-occurrence was observed among patients without an MCD-like genotype (n = 329; *P* = 0.003) (Fig. 5B).

MYC is the third lesion of the axis and behaved differently from the other two. As a clinical variable it was the weakest: single-hit *MYC* was present in only 17 responders (7 events in the 0–18-month window), its effect was strongest in that window, and it did not survive multivariable adjustment (adjusted HR 2.02, 95% CI 0.48–8.59, *P* = 0.34) (Table 1, Model 3). Failure rates were nonetheless higher at every time point (0–18 months: 41.2% vs 12.2% for *MYC* wild-type; Fig. 6C).

We examined the mutational mechanism. Restricting to the 687 DLBCL samples in our sequencing series that had sequence-context information and a C > T/G > A transition, mutations in *MYC* were enriched for the WRCY motif that defines activation-induced cytidine deaminase (AID) off-target activity: 46.1% of *MYC* transitions occurred in a WRCY context versus 34.0% background (OR 1.69, 95% CI 1.16–2.45, *P* = 0.007 by Fisher's exact test). Counting each genomic position once removes the inflation produced by recurrence at a single hotspot; on that measure *MYC* remained clearly above background (37.8% vs 19.5%, OR 2.63, 95% CI 1.62–4.26, *P* < 0.001, 74 unique positions) and comparable to canonical AID targets such as *IRF4*, ID3, *ITPKB* and *MFHAS1* (Fig. 6A). *PIM1* was the most AID-like gene on the per-mutation measure (52.1%) and fell to 21.4% per position, showing how recurrence distorts the two calibres (Fig. 6B). *MYC* mutation in this disease also carries the imprint of the same off-target mutational process that generates the other lesions of the axis.

Robustness and specificity

After adjustment, the models separate the two windows (Table 1): in the early window *TP53* mutation was independently associated with failure (n = 423; Model 3 adjusted HR 3.20, 95% CI 1.65–6.22) and *CDKN2A* loss was not (HR 1.42, 95% CI 0.60–3.37, *P* = 0.42); in the late window the pattern reversed (*CDKN2A* HR 4.38, 95% CI 1.68–11.44; *TP53* HR 1.01). Adding IPI and stage gave a similar *TP53* estimate (HR 3.28, 95% CI 1.72–6.28).

The findings held across sensitivity analyses. Bootstrap, permutation and leave-one-out analyses preserved the direction of each effect (Figure S2); no other marker or mutated gene reached a 5% false discovery rate (Figure S3); moving the endpoint boundary from 9 to 21 months (HR 2.65 to 1.92; all *P* < 0.05; Figure S4A) and sliding the 12-month *CDKN2A* window across follow-up (HR 1.94 to 9.89; all *P* < 0.05; Figure S4B) left the associations significant; and the *CDKN2A* late-window effect was stronger in patients treated with R-CHOP or R-CHOP-like regimens (HR 8.66, 95% CI 3.33–22.50; Figure S4C). p53 immunohistochemistry detected *TP53* mutation with 58.2% sensitivity and 82.8% specificity (Table S7, Figure S5).

Among the 52 patients with primary refractoriness, *TP53* mutation was over-represented (21/52, 40.4%, vs 99/484, 20.5%; OR 2.63, *P* = 0.002), and *CDKN2A* loss and single-hit *MYC* showed no enrichment.

Discussion

CDKN2A deletion and *TP53* mutation were reported to be mutually exclusive in MCD DLBCL in 2021 [13], and an earlier, smaller study reached the opposite conclusion [14]. The present analysis places the exclusivity on the axis itself and adds evidence that the two lesions mark different periods of failure after first-line therapy. In this cohort *TP53* mutation was associated with failure confined to the first year and *CDKN2A* loss with failure confined to the second, with each lesion null in the other's window, and the same double pattern appeared within a single multivariable framework (Table 1).

The *CDKN2A* effect extends across the second year: both windows beginning at 12 months were significant, and the 12–18-month band carries the largest estimate (HR 9.89). Subtype and cell of origin left the pattern intact: subtype did not predict failure timing, stratification left both effects unchanged, and the pattern replicated within non-GCB and GCB disease. The exclusivity reproduced in four independent datasets and held outside MCD-like genotypes as strongly as inside, reproducing the published subtype association [13].

TP53 mutation has long been known to identify a poor-prognosis group under R-CHOP [6], and *CDKN2A* deletion has been independently adverse since 2010 [7], with recent confirmation [8]. Both lesions are prognostic in analyses that ignore timing. The window-specific comparison presented here adds the timing dimension: the two lesions act in different years. The mutual exclusivity reported within MCD [13] has been read as a subtype-restricted phenomenon; our data place the restriction on the axis itself. Single-hit *MYC* was present in only 17 responders and its association did not survive adjustment, but its mutational data place it within the same AID-driven off-target process that generates the rest of the axis [23]. The same exclusivity is read as shared-module redundancy in other tumours [24, 25]. A recent integrated analysis of *TP53*-mutant DLBCL reported that adding ibrutinib to R-CHOP improves progression-free survival in this group [26], which illustrates why timing matters: a *TP53*-directed first-line strategy is, in effect, an early-window strategy. That the same genotype also predicts benefit from a targeted agent means that *TP53*-mutant disease can respond, and genotype-directed trials in this axis — including the MCD- and N1-restricted benefit seen with ibrutinib in the Phoenix analysis [27] — will need to account for the period in which risk falls.

Several limitations bear on interpretation. The cohort is single-centre and follow-up is short: median follow-up in responders was 14.0 months, so the 12–24-month window rests on 255 patients and the *CDKN2A* late-window estimate on 38 patients with loss. The *TP53* interaction test rests on four late-window events; the head-to-head difference remained significant (*P* = 0.027 in the joint model; *P* = 0.012 by the ratio of window-specific HRs). Progression-free survival records progression or relapse only; deaths were not captured, so the endpoint is time to progression. The local caller reports a binary loss call without a ratio, so loss of any kind is the primary definition (Table S1). IPI and Ann Arbor stage were

missing in about a quarter of patients. The design is observational, and the cross-cohort analysis tests co-occurrence.

Two implications follow. For surveillance, a *CDKN2A*-deleted patient who is progression-free at 12 months enters a period of elevated risk, which argues against relaxing follow-up after a clean first year. For trial design, pooling *TP53* and *CDKN2A* lesions mixes patients whose risk is concentrated at different times; matching the intervention window to the lesion could change the result.

In summary, in a single-centre DLBCL cohort, *TP53* mutation and *CDKN2A* deletion were mutually exclusive — a property that replicated in four independent cohorts and held outside MCD — and their prognostic signals were concentrated in the first and second years after first-line therapy respectively, a pattern that is consistent across sensitivity analyses and supported by a significant difference between the two lesions in when they acted ($P = 0.027$ in the joint model; $P = 0.012$ by the ratio of window-specific HRs).

Declarations

Ethics approval.

This study was approved by the Ethics Committee of the Cancer Hospital, Chinese Academy of Medical Sciences (CHCAMS; Approval No. 22/031-3232). The requirement for informed consent was waived by the Ethics Committee due to the retrospective nature of the study and the use of anonymized patient data. The study was conducted in accordance with the Declaration of Helsinki.

Consent to participate.

Not applicable; the requirement for written informed consent was waived by the Ethics Committee as described above.

Conflicts of interest.

The authors declare no competing interests.

Use of artificial intelligence tools.

A large language model was used during preparation of this manuscript solely to improve the language and readability of the text. All authors reviewed and verified the content and take responsibility for it.

Funding.

This work was supported by the National Natural Science Foundation of China (82403823), and the Cooperation Fund of CHCAMS (CFA202503016).

Author contributions.

JLZ, FSZ and YNL were joint first authors and were responsible for data collection, data analysis and writing of the manuscript. ZTF, XJC and XMX contributed to data collection and data curation. XLF, JMY and TQ provided strategic direction and guidance and critically revised the manuscript.

Data availability.

Patient-level clinical and genomic data are not publicly available because they contain information that could compromise participant privacy, but are available from the corresponding author on reasonable request and subject to institutional data-sharing policy. For access to raw data, please contact Tian Qiu (qiutian@cicams.ac.cn). Public datasets analysed here (dlbcl_duke_2017, mbn_msk_2024, dlbc_tcga_pan_can_atlas_2018 and pcnsl_msk_2024) were retrieved from cBioPortal (https://www.cbioportal.org) [18] and remain subject to the access terms of the original studies.

References

1. Coiffier B, Lepage E, Briere J, Herbrecht R, Tilly H, Bouabdallah R, et al. CHOP chemotherapy plus rituximab compared with CHOP alone in elderly patients with diffuse large-B-cell lymphoma. N Engl J Med. 2002;346(4):235–42.
2. Sehn LH, Salles G. Diffuse large B-cell lymphoma. N Engl J Med. 2021;384(9):842–58.
3. Maurer MJ, Ghesquières H, Jais JP, Witzig TE, Haioun C, Thompson CA, et al. Event-free survival at 24 months is a robust end point for disease-related outcome in diffuse large B-cell lymphoma treated with immunochemotherapy. J Clin Oncol. 2014;32(10):1066–73.
4. Bock AM, Mwangi R, Wang Y, Khurana A, Maurer MJ, Ayers A, et al. Defining primary refractory large B-cell lymphoma. Blood Adv. 2024;8(13):3402–15.
5. Hilton LK, Ngu HS, Collinge B, Dreval K, Ben-Neriah S, Rushton CK, et al. Relapse timing is associated with distinct evolutionary dynamics in diffuse large B-cell lymphoma. J Clin Oncol. 2023;41(25):4164–77.
6. Xu-Monette ZY, Wu L, Visco C, Tai YC, Tzankov A, Liu WM, et al. Mutational profile and prognostic significance of TP53 in diffuse large B-cell lymphoma patients treated with R-CHOP: report from an International DLBCL Rituximab-CHOP Consortium Program Study. Blood. 2012;120(19):3986–96.
7. Jardin F, Jais JP, Molina TJ, Parmentier F, Picquenot JM, Ruminy P, et al. Diffuse large B-cell lymphomas with CDKN2A deletion have a distinct gene expression signature and a poor prognosis under R-CHOP treatment: a GELA study. Blood. 2010;116(7):1092–104.

8. Ma WY, Shao LT, Tian WX, Liu S, Li Y. Prognostic value of CDKN2A copy number deletion in patients with diffuse large B-cell lymphoma. Zhongguo Shi Yan Xue Ye Xue Za Zhi. 2025;33(2):379–86.
9. Xu-Monette ZY, Deng Q, Manyam GC, Tzankov A, Li L, Xia Y, et al. Clinical and biologic significance of MYC genetic mutations in de novo diffuse large B-cell lymphoma. Clin Cancer Res. 2016;22(14):3593–605.
10. Chapuy B, Stewart C, Dunford AJ, Kim J, Kamburov A, Redd RA, et al. Molecular subtypes of diffuse large B cell lymphoma are associated with distinct pathogenic mechanisms and outcomes. Nat Med. 2018;24(5):679–90.
11. Wright GW, Huang DW, Phelan JD, Coulibaly ZA, Roulland S, Young RM, et al. A probabilistic classification tool for genetic subtypes of diffuse large B cell lymphoma with therapeutic implications. Cancer Cell. 2020;37(4):551–68.e14.
12. Ren W, Wan H, Own SA, Berglund M, Wang X, Yang M, et al. Genetic and transcriptomic analyses of diffuse large B-cell lymphoma patients with poor outcomes within two years of diagnosis. Leukemia. 2024;38(3):610–20.
13. Olszewski AJ, Sharaf R, Marcus C, Kurt H, Albacker LA, Vergilio JA, et al. CDKN2A deletions define an unfavorable subgroup within the MYD88/CD79B (MCD) subtype of diffuse large B-cell lymphoma (DLBCL) and are mutually exclusive with TP53 mutations. Blood. 2021;138(Supplement 1):2392.
14. Møller MB, Ino Y, Gerdes AM, Skjødt K, Louis DN, Pedersen NT. Aberrations of the p53 pathway components p53, MDM2 and CDKN2A appear independent in diffuse large B cell lymphoma. Leukemia. 1999;13(3):453–9.
15. Ganguli P, Basanta CC, Acha-Sagredo A, Misetic H, Armero M, Mendez A, et al. Context-dependent effects of CDKN2A and other 9p21 gene losses during the evolution of esophageal cancer. Nat Cancer. 2025;6(1):158–74.
16. Cox DR. Regression models and life-tables. J R Stat Soc Ser B. 1972;34(2):187–202.
17. Kaplan EL, Meier P. Nonparametric estimation from incomplete observations. J Am Stat Assoc. 1958;53(282):457–81.
18. Cerami E, Gao J, Dogrusoz U, Gross BE, Sumer SO, Aksoy BA, et al. The cBio cancer genomics portal: an open platform for exploring multidimensional cancer genomics data. Cancer Discov. 2012;2(5):401–4.
19. Reddy A, Zhang J, Davis NS, Moffitt AB, Love CL, Waldrop A, et al. Genetic and functional drivers of diffuse large B cell lymphoma. Cell. 2017;171(2):481–94.e15.
20. Zhu ML, Drill E, Joffe E, Salles G, Delgado AR, Zelenetz A, et al. Validation of LymphGen classification on a 400-gene clinical next-generation sequencing panel in diffuse large B-cell lymphoma: real-world experience from a cancer center. Haematologica. 2024;109(7):2326–30.
21. Hoadley KA, Yau C, Hinoue T, Wolf DM, Lazar AJ, Drill E, et al. Cell-of-origin patterns dominate the molecular classification of 10,000 tumors from 33 types of cancer. Cell. 2018;173(2):291–304.e6.
22. Grommes C, Nandakumar S, Schaff LR, Gavrilovic I, Kaley TJ, Nolan CP, et al. A phase II study assessing long-term response to ibrutinib monotherapy in recurrent or refractory CNS lymphoma.

Clin Cancer Res. 2024;30(18):4005–15.

23. Pasqualucci L, Neumeister P, Goossens T, Nanjangud G, Chaganti RS, Küppers R, et al. Hypermutation of multiple proto-oncogenes in B-cell diffuse large-cell lymphomas. Nature. 2001;412(6844):341–6.
24. Fulci G, Labuhn M, Maier D, Lachat Y, Hausmann O, Hegi ME, et al. p53 gene mutation and ink4a-arf deletion appear to be two mutually exclusive events in human glioblastoma. Oncogene. 2000;19(33):3816–22.
25. Kannan K, Munirajan AK, Krishnamurthy J, Bhuvarahamurthy V, Mohanprasad BK, Panishankar KH, et al. The p16INK4alpha/p19ARF gene mutations are infrequent and are mutually exclusive to p53 mutations in Indian oral squamous cell carcinomas. Int J Oncol. 2000;16(3):585–90.
26. Uppal M, Bhinder B, Marderstein AR, Lee Batlevi C, Falchi L, Hamlin P, et al. Integrative molecular analysis reveals determinants of clinical outcomes in TP53-mutated diffuse large B-cell lymphoma. J Clin Oncol. 2026;44(21):2029–47.
27. Wilson WH, Wright GW, Huang DW, Hodkinson B, Balasubramanian S, Fan Y, et al. Effect of ibrutinib with R-CHOP chemotherapy in genetic subtypes of DLBCL. Cancer Cell. 2021;39(12):1643–53.e3.

Figures

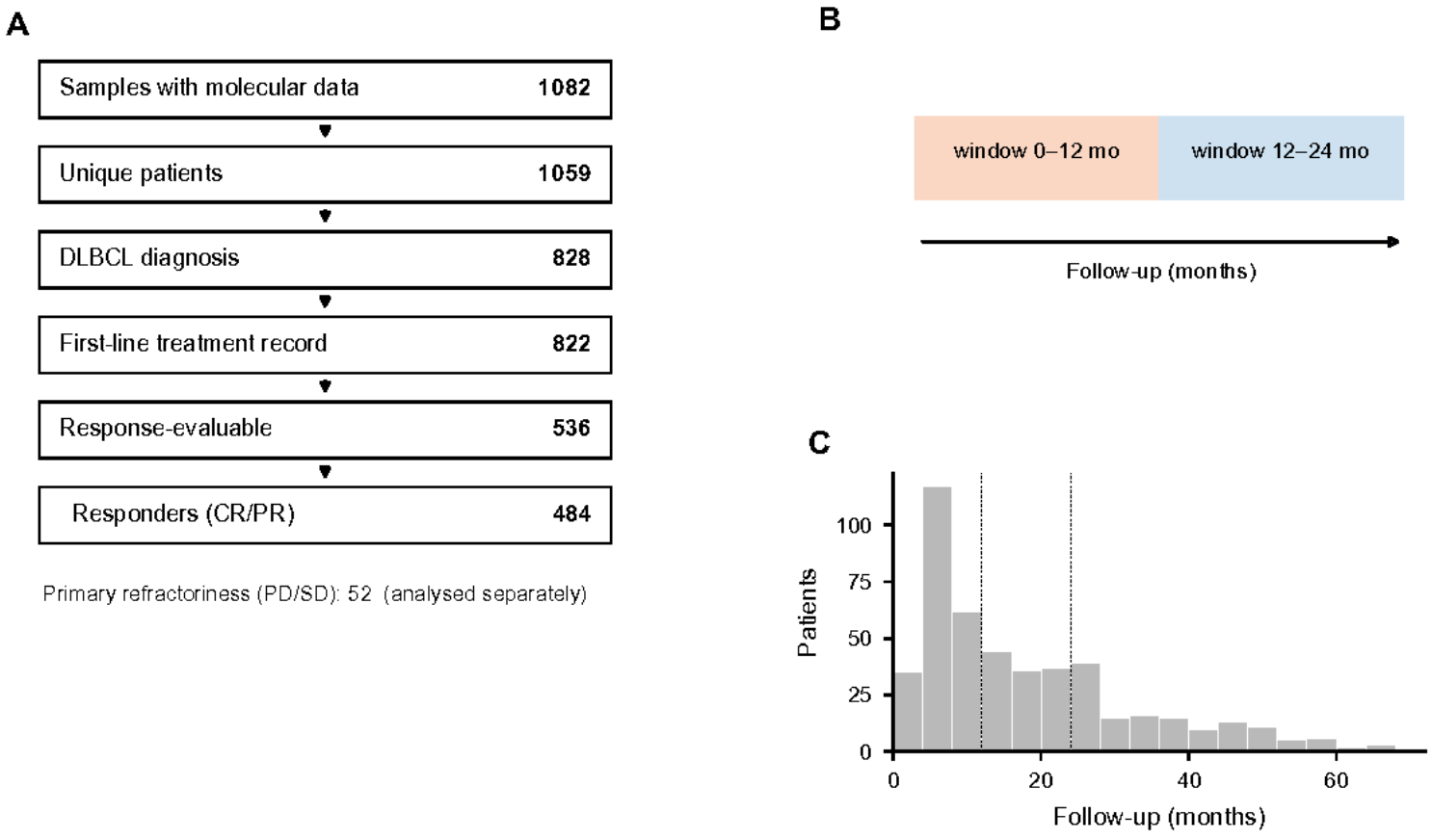

Figure 1

Study design and cohort.

(A) Cohort construction from 1 082 samples with molecular data: 828 patients with DLBCL, of whom 822 had a first-line treatment record, to the 484-responder primary analysis set, with the primary-refractory subset shown. (B) Schematic of the segmented failure-window design: each window is analysed on its own risk set, with follow-up rescaled to the window start. PTR, primary treatment refractoriness. (C) Distribution of follow-up in responders.

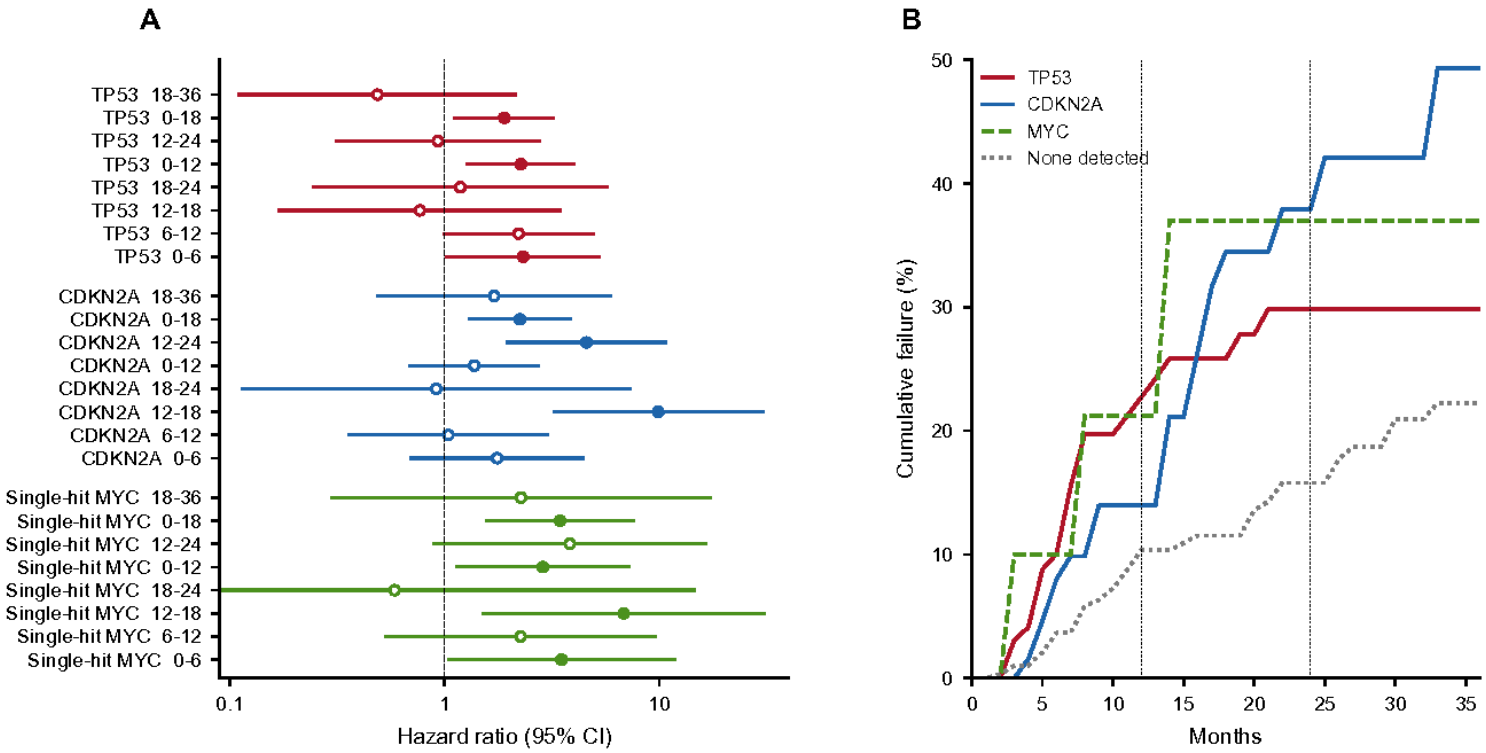

Figure 2

Lesion-specific failure windows.

(A) Hazard ratios with 95% confidence intervals for *TP53*mutation, *CDKN2A* deletion and single-hit *MYC* in eight windows (0–6, 6–12, 12–18, 18–24, 0–12, 12–24, 0–18, 18–36 months). Each window uses its own risk set. Filled symbols indicate $P<0.05$. (B) Cumulative incidence of failure by dominant lesion, assigned in priority order (*TP53*mutation > *CDKN2A* deletion > single-hit *MYC* > none detected). "No lesion detected" denotes patients who were wild-type for all three lesions.

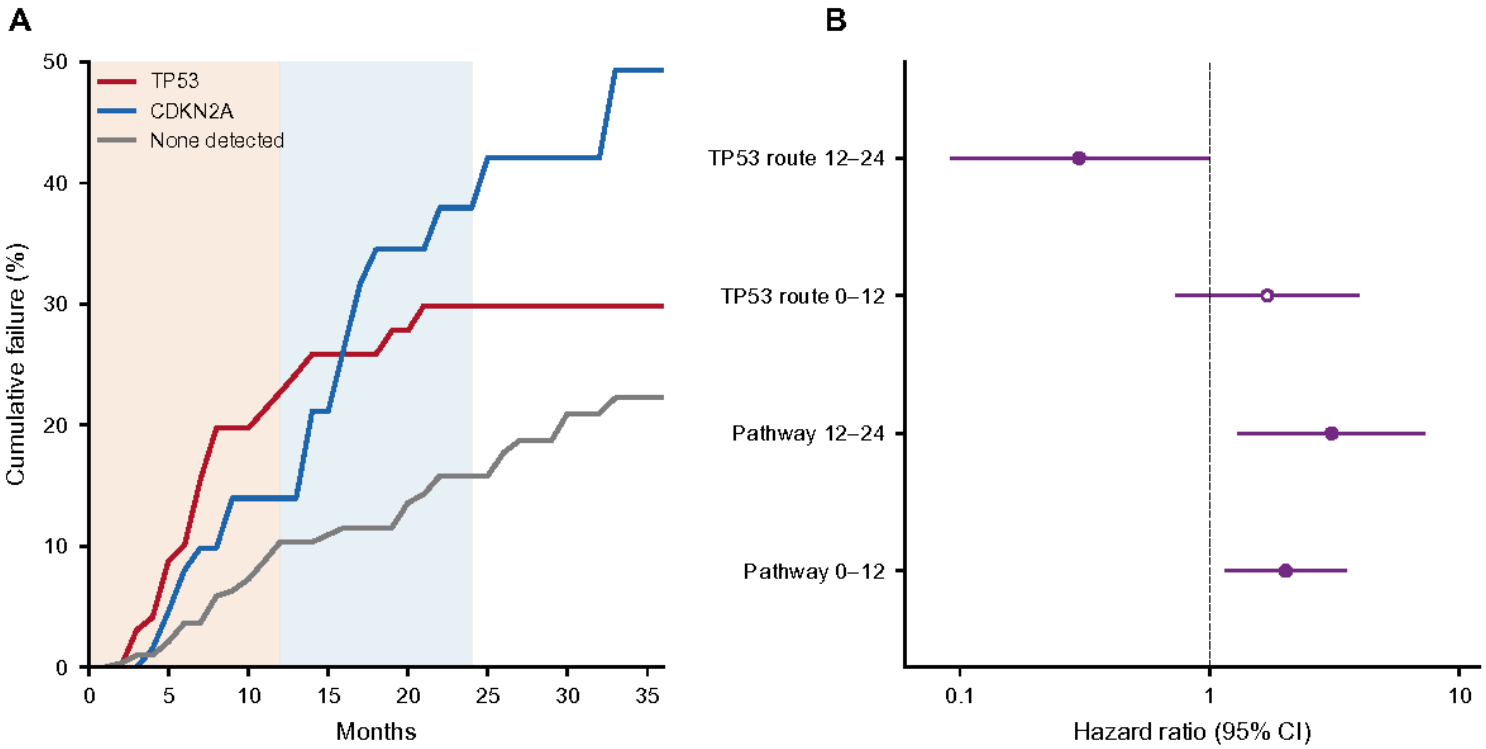

Figure 3

Complementarity and route.

(A) Cumulative incidence of failure for *TP53*-mutated, *CDKN2A*-deleted and lesion-negative patients, with the early (0–12 month) and late (12–24 month) windows shaded. (B) Among the 168 responders with at least one lesion of the axis, pathway-level disruption (either lesion) predicted failure in both windows (0–12 months: HR 2.02, *P*=0.011; 12–24 months: HR 3.08, *P*=0.009), and the identity of the lesion determined when that risk fell: the *TP53* route carried the risk in the early window and the *CDKN2A*-only route carried it in the late window (12–24 months: HR 0.30 for the *TP53* route, *P*=0.045).

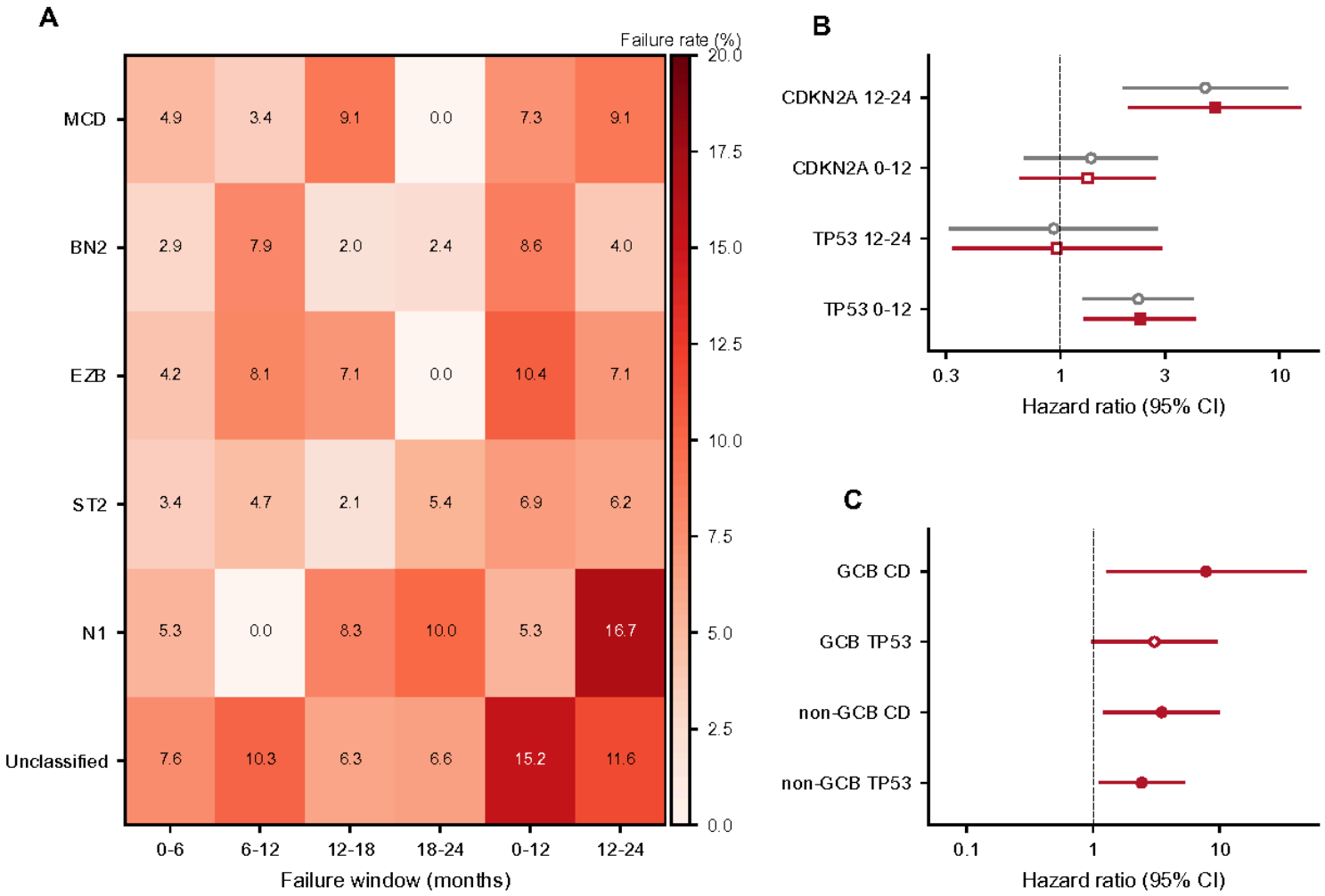

Figure 4

Independence from genetic subtype and cell of origin.

(A) Failure rate (%) by approximated LymphGen subtype and window; "–" indicates a window in which the subtype had no events or no patients at risk. (B) Hazard ratios for the two primary findings before (grey circles) and after (red squares) stratification of the Cox model by approximated LymphGen subtype. (C) Lesion effects within cell-of-origin strata. Filled symbols indicate $P<0.05$.

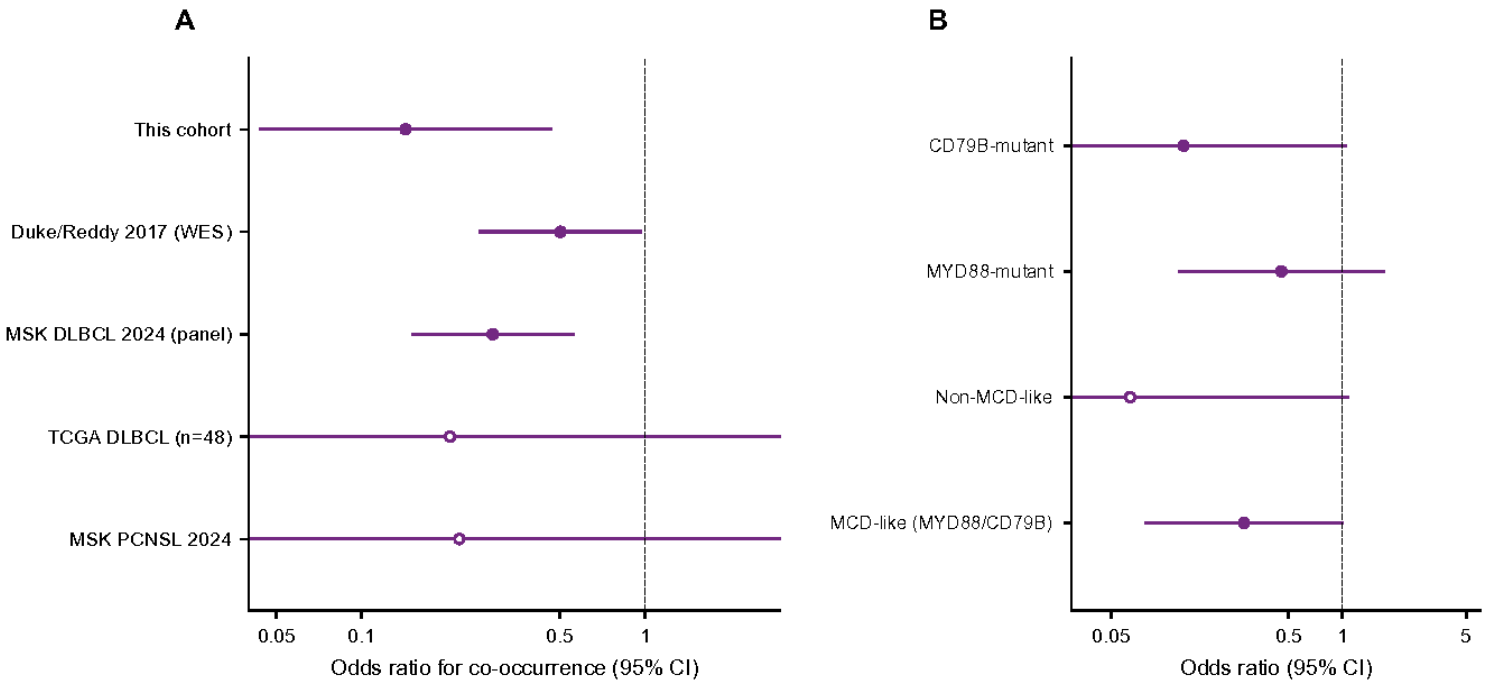

Figure 5

Mutual exclusivity of *TP53* mutation and *CDKN2A*loss.

(A) Odds ratios for co-occurrence in this cohort (484 responders) and in four independent public datasets. Arrows denote cohorts with no observed co-occurrence. All estimates lie below unity. (B) Odds ratios within and outside MCD-like genotype (*MYD88*- or *CD79B*-mutated), with *MYD88*-mutant and *CD79B*-mutant subgroups shown separately, computed in the same 484 patients. Filled symbols indicate $P<0.05$.

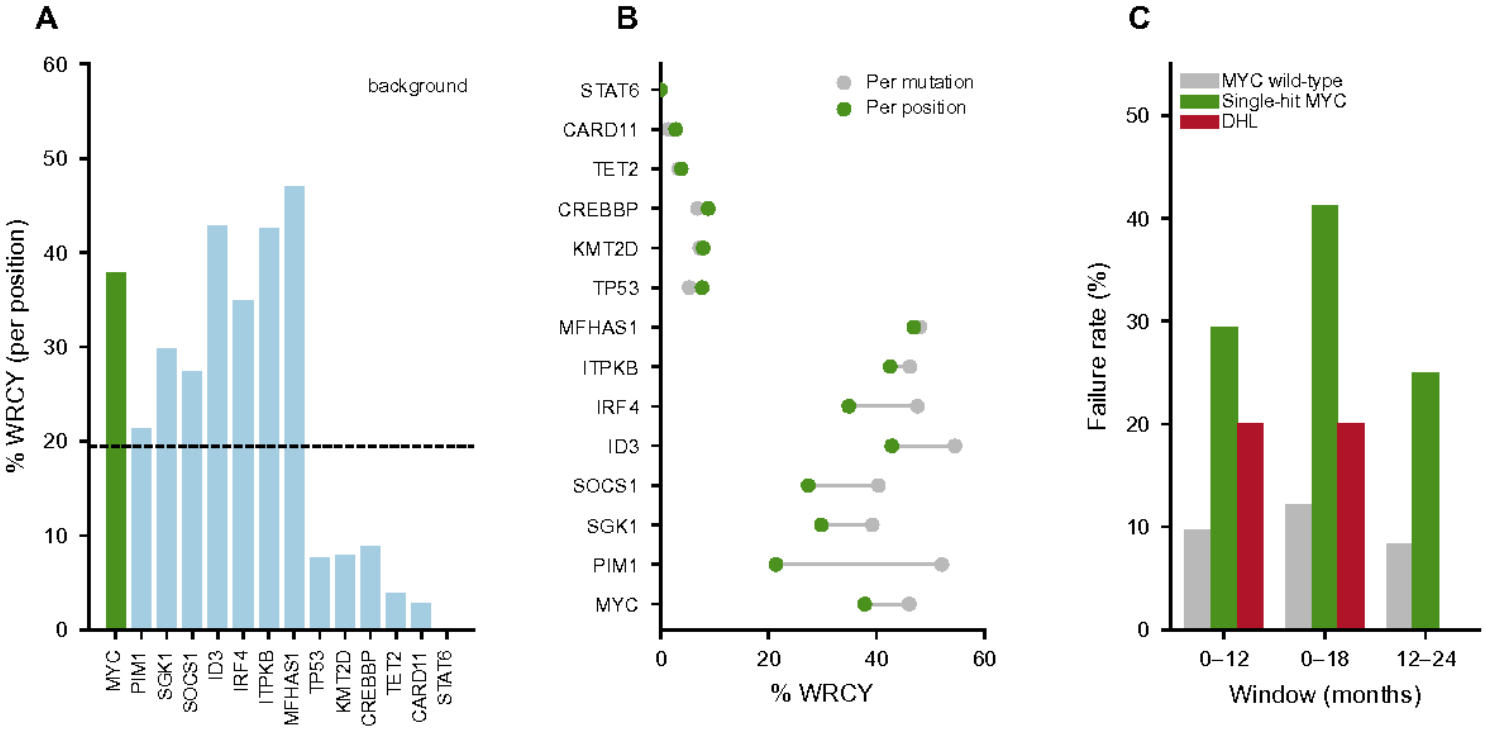

Figure 6

MYC: AID-type mutational signature and failure timing.

(A) Proportion of C>T/G>A transitions occurring in a WRCY motif, counted once per genomic position (recurrence-independent), restricted to DLBCL samples. Dashed line: background rate. (B) The same statistic computed per mutation and per unique position, illustrating why the per-mutation calibre is unreliable when recurrence is present; *PIM1*falls from 52.1% to 21.4%. (C) Failure rate by *MYC* status at 0–12, 0–18 and 12–24 months, with the number of patients at risk annotated. Single-hit *MYC*was present in 17 responders.

Supplementary Files

This is a list of supplementary files associated with this preprint. Click to download.

- TableS4allwindows.xlsx
- TableS2analysissets.xlsx
- TableS1CDKN2Adefinitionsensitivity.xlsx
- FigureS4sensitivity.pdf
- TableS5interactionandmultiplicity.xlsx
- Table1multivariablemodels.xlsx
- FigureS2resampling.pdf
- FigureS1power.pdf
- TableS7p53IHC.xlsx
- FigureS5p53IHC.pdf
- TableS3baseline.xlsx
- FigureS3specificityscreens.pdf
- TableS6exclusivitycells.xlsx